Since January 2020 Elsevier has created a COVID-19 resource centre with free information in English and Mandarin on the novel coronavirus COVID-19. The COVID-19 resource centre is hosted on Elsevier Connect, the company's public news and information website.

VIROLOGY 230, 309–322 (1997)
ARTICLE NO. VY978503

Efficient Autoproteolytic Processing of the MHV-A59 3C-like Proteinase from the Flanking Hydrophobic Domains Requires Membranes

JOSEFINA D. PIÑÓN, RAVI R. MAYREDDY, JULIE D. TURNER,[1] FARAH S. KHAN, PEDRO J. BONILLA,[2] and SUSAN R. WEISS[3]

Department of Microbiology, University of Pennsylvania School of Medicine, Philadelphia, Pennsylvania 19104-6076

Received November 5, 1996; returned to author for revisions December 10, 1996; accepted February 17, 1997

The replicase gene of the coronavirus MHV-A59 encodes a serine-like proteinase similar to the 3C proteinases of picornaviruses. This proteinase domain is flanked on both sides by hydrophobic, potentially membrane-spanning, regions. Cell-free expression of a plasmid encoding only the 3C-like proteinase (3CLpro) resulted in the synthesis of a 29-kDa protein that was specifically recognized by an antibody directed against the carboxy-terminal region of the proteinase. A protein of identical mobility was detected in MHV-A59-infected cell lysates. *In vitro* expression of a plasmid encoding the 3CLpro and portions of the two flanking hydrophobic regions resulted in inefficient processing of the 29-kDa protein. However, the efficiency of this processing event was enhanced by the addition of canine pancreatic microsomes to the translation reaction, or removal of one of the flanking hydrophobic domains. Proteolysis was inhibited in the presence of *N*-ethylmaleimide (NEM) or by mutagenesis of the catalytic cysteine residue of the proteinase, indicating that the 3CLpro is responsible for its autoproteolytic cleavage from the flanking domains. Microsomal membranes were unable to enhance the *trans* processing of a precursor containing the inactive proteinase domain and both hydrophobic regions by a recombinant 3CLpro expressed from *Escherichia coli.* Membrane association assays demonstrated that the 29-kDa 3CLpro was present in the soluble fraction of the reticulocyte lysates, while polypeptides containing the hydrophobic domains associated with the membrane pellets. With the help of a viral epitope tag, we identified a 22-kDa membrane-associated polypeptide as the proteolytic product containing the amino-terminal hydrophobic domain.

INTRODUCTION

The murine coronavirus, mouse hepatitis virus strain A59 (MHV-A59), has a positive-stranded RNA genome that is approximately 31 kb long (Bonilla *et al.,* 1994). Viral replication begins with the translation of the genomic RNA upon entry into permissive cells. This results in the production of the viral RNA-dependent RNA polymerase that is believed to be encoded in gene 1 at the 5′ end of the viral genome (Bonilla *et al.,* 1994; Lee *et al.,* 1991). Approximately 70% of the coding potential of the viral genome is contained within the two overlapping open reading frames (ORF 1a and ORF 1b) of this first locus (Bonilla *et al.,* 1994; Bredenbeek *et al.,* 1990). Together, translation of ORFs 1a and 1b via a frameshift mechanism could result in a polyprotein of greater than 800 kDa. Several functional domains are predicted to reside within these two ORFs (Bonilla *et al.,* 1994; Herold *et al.,* 1993; Lee *et al.,* 1991). The predicted RNA-dependent RNA polymerase motif (SDD) is encoded in ORF 1b along with helicase and zinc finger motifs. ORF1a encodes three predicted proteinase domains. Two are cysteine proteinases (PLP-1 and PLP-2) that are distantly related to the cellular proteinase papain, and the third is a poliovirus 3C-like proteinase (3CLpro). A growth-factor-like region is also predicted to be encoded at the 3′ end of ORF 1a. Several potential proteinase cleavage sites have been identified throughout both ORFs, suggesting that the polyprotein products of gene 1 are processed by these viral-encoded proteinases to generate individual polypeptide products (Lee *et al.,* 1991). It has been shown that the inhibition of proteolytic activity results in the rapid shutoff of MHV RNA synthesis (Kim *et al.,* 1995). The proteolytic processing of the gene 1 polyprotein, therefore, is essential for MHV replication.

The 3CLpro domain is present in all coronavirus genomes studied to date (Bonilla *et al.,* 1994; Boursnell *et al.,* 1987; Eleouet *et al.,* 1995; Herold *et al.,* 1993; Lee *et al.,* 1991). The 3CLpro spans a 303-amino acid region, between Ser3334 and Glu3636, and is flanked by two hydrophobic, and potentially membrane-spanning, domains (Bonilla *et al.,* 1994; Lee *et al.,* 1991; Lu *et al.,* 1995). At its junctions with these hydrophobic regions (HD1 and HD2) are glutamine-serine (QS) dipeptides which resemble the known cleavage sites of the picornavirus 3C proteinases. Additional 3CLpro cleavage sites were predicted to flank the polymerase, helicase, and

[1] Current address: Department of Medicine, Division of Hematology and Oncology, University of Pennsylvania School of Medicine, Philadelphia, PA 19104.

[2] Current address: Division of Molecular Virology, One Baylor Plaza, Baylor College of Medicine, Houston, TX 77030.

[3] To whom correspondence and reprint requests should be addressed. E-mail: weisssr@mail.med.upenn.edu.

0042-6822/97 $25.00

growth-factor-like regions at their junctions with other protein domains (Fig. 1). Several of these predicted sites have recently been demonstrated to be cleaved by the 3CLpro of several coronaviruses (Grotzinger *et al.,* 1996; Lu *et al.,* 1995; Tibbles *et al.,* 1996; Ziebuhr *et al.,* 1995). These observations suggest an important role for the 3CLpro in the maturation of these domains into functional proteins.

We have investigated the processing activity of the MHV-A59 3CLpro using an *in vitro* transcription–translation system. In our studies, we made use of a pET21-based plasmid that encodes most of the amino-terminal hydrophobic domain (HD1), the entire 3CLpro domain, and approximately one-half of the carboxy-terminal hydrophobic domain (HD2). A 29-kDa protein, representing the 3CLpro, can be efficiently released from the flanking hydrophobic sequences, but only if the *in vitro* reactions are supplemented with canine microsomal membranes. This 29-kDa proteinase can also be identified in lysates from MHV-A59-infected cells. The requirement for membranes is not surprising, given the hydrophobic nature of the sequences flanking the proteinase domain (see Fig. 5A). The IBV 3C-like proteinase has recently been reported to require microsomal membranes for processing activity *in vitro* (Tibbles *et al.,* 1996). In contrast, recent studies on the *in vitro* activity of the MHV-A59 3CLpro did not report a requirement for membranes (Lu *et al.,* 1996, 1995). We show here that the membrane requirement is related to the presence of the two flanking hydrophobic domains. We have also expressed the MHV-A59 3CLpro in *E. coli* and have used the partially purified recombinant fusion proteinase in *in vitro trans* cleavage assays using radiolabeled precursors generated by transcription–translation as substrates for the proteinase. Unlike the autocatalytic *cis* processing observed during transcription–translation, posttranslational *trans* cleavage of precursors containing an inactive 3CLpro, as well as portions of both hydrophobic domains, was not dependent on membranes.

MATERIALS AND METHODS

Cells and virus

DBT cells were maintained in Dulbecco's modified eagle medium supplemented with 10% fetal calf serum (DMEM/10% FCS). The MHV-A59 isolate used in this study was originally provided by Dr. Julian Leibowitz (College Station, TX).

Antisera

Rabbit antiserum UP313 and preimmune serum were raised by Cocalico (Reamstown, PA). Antiserum UP313 is directed against the peptide 3618-EDELTPSDVYQQ-LAGVKLQ-3636, corresponding to the carboxy-terminal-most 19-amino acid residues of the predicted 3CLpro domain (Bonilla *et al.,* 1994; Lee *et al.,* 1991). Preimmune serum was also collected from rabbits. These antibodies were partially purified by passage through a protein A–Sepharose CL-45 column. The sera were diluted in Tris–saline buffer (50 m*M* Tris, pH 8.6, 150 m*M* NaCl, 0.02% sodium azide) and applied to the column. Unbound proteins were removed by washing the column with 50 m*M* Tris–HCl buffer, pH 7.2. Antibodies were eluted with 0.1 *M* citric acid (pH 3.0), neutralized with 1 *M* Tris, and dialyzed in 1× phosphate-buffered saline, pH 7.2 (20 m*M* sodium phosphate, 150 m*M* NaCl). Protein concentration was determined by UV spectroscopy.

The antipeptide antibody 12CA5 is directed against the epitope YPYDVPDYA derived from the influenza virus hemaglutinin (HA) protein (Kolodziej and Young, 1991). The murine ascites fluid containing this antiserum (BAbCO) was provided by Dr. Michael Malim (Philadelphia, PA).

Plasmids

The plasmids used in this study are illustrated in Figs. 1C and 5A. The cDNA 917–919b (Pachuk *et al.,* 1989) had been previously cloned into pACYC5.3 to yield the plasmid pACYC 5.3-917/919. An *Spe*I–*Sac*I fragment from pACYC 5.3-917/919 was cloned into the *Nhe*I and *Sac*I sites of pET21a (Novagen), resulting in pET21-HD1.3C.HD2. This plasmid encodes ORF 1a amino acids from Ser3149 to Leu3783.

The plasmid pET21-3C was constructed by polymerase chain reaction (PCR) amplification of the predicted 3CLpro domain using pET21-HD1.3C.HD2 as the template and the primers F3CP (5′-GGAATTCCATATGTCTGGTATAGTG-AAGATG-3′) and R3CP (5′-GAATTCCTCGAGTTACTGTAG-CTTGACACCAGCTAG) which introduces the restriction sites for *Nde*I and *Ava*I at the 5′ and 3′ ends of the amplified product, respectively, as denoted by the underlined letters in the primer sequences. The PCR fragment was digested with *Nde*I and *Ava*I and cloned into the corresponding sites in the pET21a vector. The resulting plasmid encodes an additional methionine residue immediately upstream of the 3CLpro coding region.

The plasmid pET21-HD1.3C.HD2 was digested with the restriction enzyme *Hin*dIII. The larger DNA fragment of approximately 7312 nucleotides was religated resulting in the plasmid pET21-HD1.3C.Hind3. This plasmid contains a 93 amino acid truncation in HD2 compared to the parental construct pET21-HD1.3C.HD2.

A region of MHV-A59 gene 1 from nucleotides 9912 to 10661 was PCR amplified from pET21-HD1.3C.HD2 using the primers FSP 9912–9930 (5′-GGAATTCCATATGGCC-AAAATTGGTACCGAGGTT-3′) and RSP 10661–10644 (5′-AACATATCCTACAGAACC-3′), digested with *Nde*I and *Bam*HI, and cloned into the corresponding sites of pET21-3C resulting in the plasmid pET21-NX.3C. An *Nde*I–*Bam*HI fragment from pET21-HD1.3C.HD2 was

subsequently subcloned into the *Nde*I and *Bam*HI sites of pET21-NX.3C to yield pET21-HD1.3C. Similarly, the region from nucleotides 10599 to 11595 of MHV-A59 ORF 1a was PCR amplified from pET21-HD1.3C.HD2 using the primers FSP 10599–10622 (5′-CGTAGTAGCCATACCATAAAGGGC-3′) and RMP 11595–11562 (5′-CCTCTTCCTCGAGATTGGCTCCAAAATACCACA-3′). Following digestion with *Bam*HI and *Ava*I, the PCR fragment was cloned into the *Bam*HI and *Ava*I sites of pET21-3C. That fragment was later replaced by a *Bam*HI–*Ava*I fragment from pET21-HD1.3C.HD2, resulting in the plasmid pET21-3C.HD2.

The coding sequences representing the MHV-A59 3CLpro domain were PCR amplified from pET21-HD1.3C.HD2 using the primers FSP 3C (5′-GCGCCGGAATTCTCTGGTATAGTGAAGATGGTGTCG-3′) and RSP 3C (5′-GCTCTAGAGCTTACTGTAGCTTGACACCAGC-3′). The PCR amplified fragment was then digested with *Eco*RI and *Xba*I (denoted by the underlined sequences in the primers) and cloned into the corresponding sites of the pMALC2 vector (New England Biolabs), resulting in the plasmid pMAL-3C.wt, which encodes the 3CLpro fused to and downstream of the maltose binding protein (MBP). The plasmid pMAL-3C.mut, encoding the 3CLpro containing the inactivating mutation C3478A, was constructed in a similar manner using the construct pET21-HD1.3C.HD2 C3478A (see below) as the template for PCR amplification.

Site-directed mutagenesis of Cys3478 to Ala

The vector pET21a-*Hin*dIII (−) was constructed by digesting the plasmid pET21a with the restriction enzyme *Hin*dIII, filling in the recessed ends using the Klenow fragment of DNA Polymerase I, and blunt-end ligation of the filled-in DNA ends. A *Bgl*II–*Sal*I fragment from pET21-HD1.3C.HD2 was cloned into the corresponding sites in pET21a-*Hin*dIII (−) resulting in the construct pET21-HD1.3C.HD2-*Hin*dIII (−).

A *Bam*HI–*Hin*dIII fragment from cDNA 917 (Pachuk *et al.,* 1989) was cloned into M13mp18 utilizing the *Bam*HI and *Hin*dIII sites in the replicative form (RF) of the DNA to give rise to the recombinant plasmid M13mp18B_2H. A 345-bp fragment containing a mutation in the catalytic cysteine was PCR amplified using the primers FMP C3478A (5′-ATGTGGATCCGCCGGTTCTGTG-3′) and RSP 10980–10959 (5′-TGGCCTGTCATAGAAGCAAGCGC-3′). This fragment was purified and digested with the restriction enzymes *Bam*HI (denoted by the underlined sequence) and *Sca*I and cloned back into the corresponding sites in M13mp18B_2H to yield M13mp18B_2H C3478A. A cysteine to alanine mutation (TGC to GCC) was confirmed by sequencing of the RF DNA. A *Bam*HI–*Hin*dIII fragment from M13mp18B_2H C3478A was cloned into the corresponding sites in pET21-HD1.3C.HD2-*Hin*dIII (−). The resulting construct was named pET21-HD1.3C.HD2 C3478A.

A region containing the C3478A mutation in the 3CLpro coding region was PCR amplified from pET21-HD1.3C.HD2 C3478A using the primers FSP 10599–10622 and R3CP. Following digestion with *Bam*HI and *Ava*I, the amplified fragment was cloned into the corresponding sites in pET21-NX.3C to yield pET21-NX.3C C3478A.

Cell infection, cell lysis, and immunoblot analysis

DBT cells were grown to confluency and infected with MHV-A59 at a multiplicity of infection of 10 PFU/cell. A parallel culture was mock infected. Syncytia formation, observed 8–9 hr postinfection, was used as a visual indicator of viral protein expression. At 9 hr postinfection the cells were collected and lysed in buffer containing 10 m*M* Tris–HCl, pH 7.4, 150 m*M* NaCl, 1% NP-40, and the proteinase inhibitors phenylmethylsulfonyl fluoride (PMSF) and aprotinin (100 and 20 μg/ml, respectively) for 10 min on ice. The intact nuclei were pelleted and the clarified extracts stored at −80°. Equal amounts of protein were analyzed by sodium dodecyl sulfate–polyacrylamide gel electrophoresis (SDS–PAGE). The separated proteins were transferred to polyvinylidene fluoride (PVDF) membranes (Millipore). The membranes were incubated in Tris-buffered saline (10 m*M* Tris–HCl, pH 8.0; 150 m*M* NaCl) containing 0.1% Tween 20 and 5% nonfat milk (TBST/milk). Following this blocking step the membranes were incubated with either antiserum UP313 or the preimmune serum as specified for each experiment. The membranes were then washed three times in 1× TBST solution without milk and then incubated with horse radish peroxidase-conjugated anti-rabbit IgG (Cappel) for another hour. Antigenically active polypeptides were visualized using phosphatase coupled antibody (ECL kit, Amersham) and exposed to X-ray film.

In vitro transcription and translation

Expression of the plasmid DNAs was carried out using the TnT rabbit reticulocyte lysate coupled transcription–translation system (Promega) as previously described (Bonilla *et al.,* 1995). Where indicated, 5 Eq of canine pancreatic microsomal preparations (Promega) was also added to the translation reaction. The cysteine proteinase inhibitor *N*-ethylmaleimide (NEM) (0.025 μg/μl) was added to the reaction where indicated to test its effect on processing. The incorporation of [^{35}S]methionine into acid precipitable counts was used as an indicator of protein synthesis. Equivalent amounts of acid precipitable counts were directly analyzed by SDS–PAGE or immunoprecipitated with UP313 prior to electrophoresis. Radioimmunoprecipitations (RIP) were carried out as described previously (Bonilla *et al.*, 1995; Denison *et al.*, 1991).

Time course analysis of processing was carried out by both pulse–labeling and pulse–chase assays.

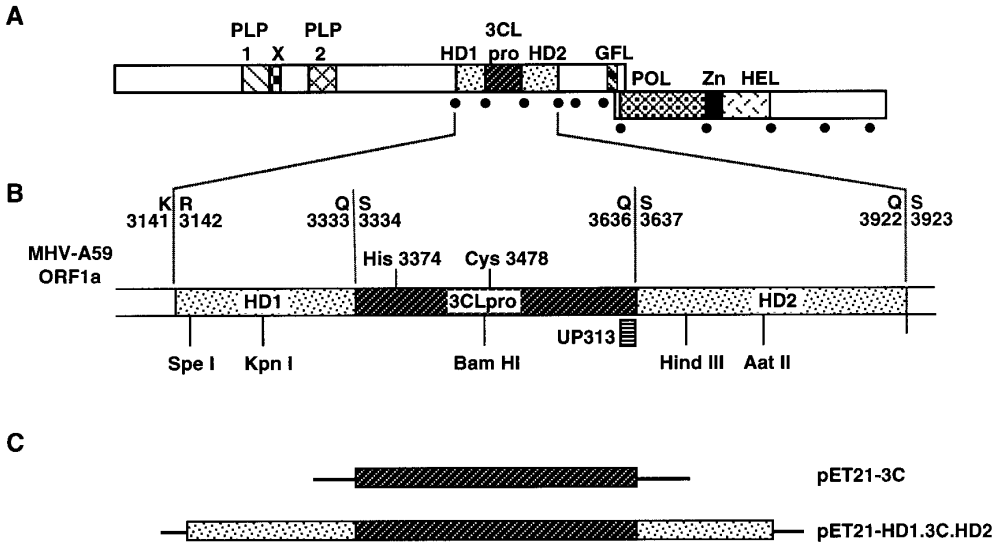

FIG. 1. Map of MHV-A59 3CLpro domain. (A) Map of ORF 1a and 1b showing the location of the predicted functional domains. The 3CLpro (▨) is located between two hydrophobic domains, HD1 and HD2 (▤). The predicted 3CLpro cleavage sites are shown as closed circles. (B) Enlarged map of the HD1-3CLpro-HD2 region showing the unique restriction sites in the region. The 3CLpro lies within the region from Ser3334 to Glu3636. The location of the catalytic residues, His3374 and Cys3478, are shown. The UP313 antiserum (▤) was raised against the last 19 amino acids of the 3CLpro. (C) pET21-3C encodes the 3CLpro downstream of the T7 promoter in the pET21a vector. pET21-HD1.3C.HD2 encodes MHV-A59 amino acid sequences from Ser3149 to Leu3783 behind the T7 promoter of pET21a.

Pulse–label reactions were performed as described above in reaction volumes of 50 μl in the absence and presence of microsomal membranes. At specific time points between 0 and 300 min, 5-μl aliquots were removed, added directly to 2× Laemli buffer, and analyzed by SDS–PAGE. When pulse–chase assays were performed, the translation reactions were terminated by the addition of cyclohexamide (0.5 μg/50-μl reaction), excess cold methionine (2 m*M*), and RNase A (0.16 μg/μl) (Bonilla *et al.,* 1997).

To determine membrane binding, plasmid DNAs were transcribed and translated in the presence of microsomes. Following translation, membranes were pelleted by centrifugation at 12,000 *g* for 15 min at 4° (Echeverri and Dasgupta, 1995) and then resuspended in 1× low salt RIP buffer (10 m*M* Tris–HCl, pH 7.4, 150 m*M* NaCl, 1% NP-40, 1% sodium deoxycholate, 1% SDS). Volumes of soluble and membrane fractions containing equivalent counts per minute were directly analyzed by SDS–PAGE. The amount of proteins analyzed in this manner were not representative of the actual ratio of proteins in the soluble versus the pellet fraction, with the proteins in the pellet fraction being slightly overrepresented. We estimated the percentage of total proteins partitioned into each fraction by calculating the amount of acid precipitable counts in each fraction as a percentage of the total acid precipitable counts of both fractions.

Overexpression and partial purification of the recombinant 3CLpro

Expression and purification of the recombinant 3CLpro were carried out according to manufacturer's instructions (New England Biolabs). Briefly, *E. coli* DH5α cells transformed with either the plasmid pMal-3C.wt or pMal-3C.mut were induced with isopropyl-thio-β-D-galactoside (IPTG) at a final concentration of 0.3 m*M* for 3–4 hr at 30°. Cells were harvested and lysed by sonication. Cell debris were pelleted by centrifugation at 9000 *g* for 30 min. The crude lysates were loaded onto an amylose column equilibrated with column buffer (20 m*M* Tris–HCl, pH 7.4, 200 m*M* NaCl, 1 m*M* EDTA, and 1 m*M* DTT) at a flow rate of 1 ml/min. The column was washed with 12 column volumes of column buffer and the MBP-3CLpro fusion protein was eluted with column buffer containing 10 m*M* maltose. The concentration of the fusion protein was estimated on a 10% SDS–polyacrylamide gel against known concentrations of bovine serum albumin (BSA) protein. The recombinant proteinase was stored at −80° in column buffer supplemented with 20% glycerol.

Posttranslation proteolytic assays

Radiolabeled substrates were generated using the TnT rabbit reticulocyte system as described above. Lysate volumes containing equivalent counts per minute were incubated with approximately 3–4 μg of the recombinant proteinase or an equivalent volume of column buffer/20% glycerol for 12–16 hr at 30°. The processed products were analyzed by SDS–PAGE.

Epitope tagging

The HA epitope derived from the influenza virus hemagglutinin (HA) protein was introduced into pET21-HD1.3C by PCR amplification of pET21-HD1.3C.HD2 using the primers

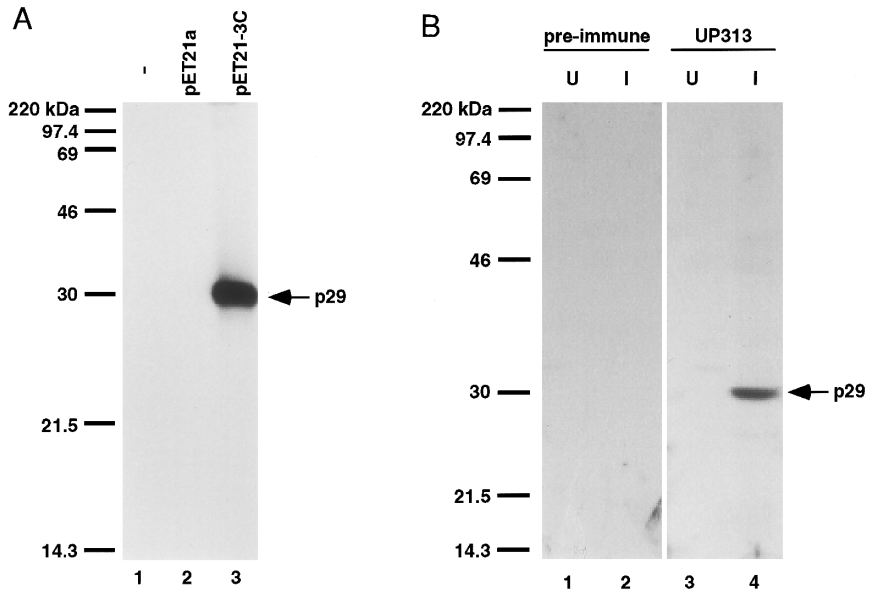

FIG. 2. Identification of 3CLpro *in vitro* and *in vivo.* (A) SDS–PAGE analysis of radiolabeled products encoded by pET21-3C. pET21-3C (lane 3) was *in vitro*-transcribed and translated as described under Material and Methods. As controls, reactions were prepared with no DNA (lane 1) or with the vector DNA, pET21a (lane 2), added to the reaction. Equivalent lysate volumes were subjected to immunoprecipitation with UP313 antiserum prior to analysis on a 15% SDS–polyacrylamide gel. (B) Detection of the 3CLpro in virus-infected cells. Uninfected (U) and infected (I) cell lysates were analyzed by Western blotting, following electrophoretic separation on a 10% SDS–polyacrylamide gel, with preimmune serum (lanes 1 and 2) and antiserum UP313 (lanes 3 and 4). The molecular mass in kilodaltons of prestained protein markers is indicated to the left of each panel. The arrows to the right of each panel indicates the electrophoretic migration of the 29-kDa 3CLpro.

FSP HA-MHV9648 (5′-GGAATTCCATATGTACCCATACGACGTCCCAGACTACGCTTACACTAGTGTTGTGGTTATCAAT-3′) and RSP 10673 (5′-ATCGCCAGTTAAAACATATCCTACAGAACC-3′). FSP HA-MHV9648 contains a 40-nucleotide overhang encoding the restriction site *Nde*I, as denoted by the underlined sequences, as well as the HA epitope, denoted by the bold-faced sequences. The PCR amplified fragment was digested with *Nde*I and *Bam*HI and cloned back into pET21-HD1.3C resulting in pET21-HA.HD1.3C. Membrane association assays were performed using this plasmid. Equivalent counts per minute from soluble and membrane fractions were immunoprecipitated with the antibody 12CA5 as previously described (Bonilla *et al.,* 1995; Denison *et al.,* 1991). Immunoprecipitated proteins were then analyzed by SDS–PAGE.

RESULTS

Identification of the 3CLpro *in vitro* and in infected cells

A plasmid encoding the core 3CLpro of MHV-A59, pET21-3C, was *in vitro*-transcribed and translated in the presence of [^{35}S]methionine. The translation products were immunoprecipitated with the antibody UP313 and analyzed by SDS–PAGE. *In vitro* expression of pET21-3C resulted in the production of a protein with an apparent migration of 29 kDa (predicted molecular weight, 33 kDa) that is immunoprecipitated by UP313 (Fig. 2A, lane 3). This 29-kDa protein (p29) is neither present in translation reactions that did not contain plasmid DNA (lane 1) nor is it present in translations of the bacterial expression vector pET21a (lane 2). The p29 protein is therefore specifically expressed from the 3CLpro encoding plasmid, pET21-3C. Since the UP313 antibody recognizes the carboxy-terminal end of the 3CLpro, p29 most likely represents the full-length 3CLpro translation product.

To determine if p29 represents the mature 3CLpro, we looked for the expression of a similar protein *in vivo.* Lysates from MHV-A59-infected cells were separated by SDS–PAGE, transferred to a PVDF membrane, and analyzed by Western blotting with UP313 (Fig. 2B). A 29-kDa protein was recognized specifically by the UP313 antibody in lysates of infected cells (lane 4), but not in uninfected cells (lane 3). Preimmune serum was unable to detect p29 in infected or uninfected cell lysates (lanes 1 and 2). These *in vivo* results provide further support that the 29-kDa protein detected in *in vitro* transcription–translation experiments represents the mature 3CLpro.

Demonstration of 3CLpro processing *in vitro*

To study the processing activity of the 3CLpro *in vitro,* we constructed the plasmid pET21-HD1.3C.HD2 (Fig. 1C). This plasmid encodes a precursor protein with a predicted molecular weight of approximately 72 kDa that contains the 3CLpro as well as the two QS sites at its junctions with the flanking hydrophobic domains. Processing at these two sites would result in the release of the 3CLpro from the flanking hydrophobic sequences.

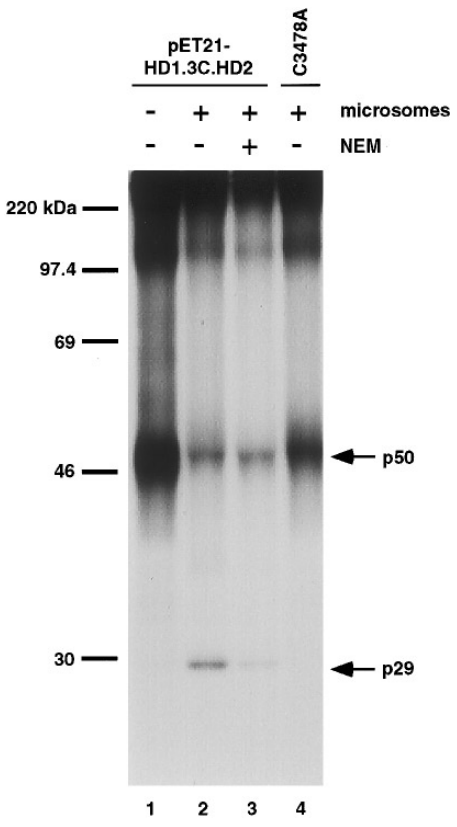

FIG. 3. Demonstration of *in vitro* processing by the 3CLpro. The plasmids pET21-HD1.3C.HD2 and pET21-HD1.3C.HD2 C3478A, containing a mutation in the catalytic cysteine residue of the proteinase, were *in vitro*-transcribed and translated in the absence or presence of canine pancreatic microsomal membranes and the cysteine proteinase inhibitor NEM. Volumes of [^{35}S]methionine-labeled lysates containing equivalent amounts of acid precipitable counts were immunoprecipitated with UP313. The immunoprecipitated products were analyzed on a 10% SDS–polyacrylamide gel. Lane 1, pET21-HD1.3C.HD2 translation in the absence of microsomes and NEM. Lane 2, pET21-HD1.3C.HD2 translation reaction supplemented with microsomes. Lane 3, pET21-HD1.3C.HD2 translation reaction in the presence of microsomes and NEM. Lane 4, pET21-HD1.3C.HD2 C3478A translation in the presence of microsomes. Molecular weight protein markers are indicated to the left. The electrophoretic migration of the full-length precursor (50 kDa) and the 3CLpro (29 kDa) are indicated on the right.

The 3CLpro could then be identified based on its molecular weight and its ability to be immunoprecipitated by the antibody UP313. *In vitro* transcription–translation reactions of the pET21-HD1.3C.HD2 plasmid by itself, however, did not result in appreciable processing of the 29-kDa 3CLpro (Fig. 3, lane 1). Only a precursor, with an apparent molecular weight of 50 kDa, was observed. Due to the hydrophobic nature of the sequences flanking the 3CLpro, we decided to perform our *in vitro* reactions in the presence of canine pancreatic microsomal membranes. The [^{35}S]methionine-labeled translation products generated from pET21-HD1.3C.HD2 in the presence of microsomal membranes were immunoprecipitated with UP313. Analysis of the immunoprecipitated products by electrophoresis revealed the production of the 29-kDa 3CLpro when the translation reaction was supplemented with microsomes (lane 2). These results suggest a requirement for microsomal membranes for the processing of the MHV-A59 3CLpro from the flanking hydrophobic regions.

The catalytic residues of the 3CLpro have been previously identified (Lu *et al.*, 1995). Amino acid residues His3374 and Cys3478 were shown to be essential for proteinase activity. Using site-directed mutagenesis a mutant of pET21-HD1.3C.HD2 was created in which the catalytic residue Cys3478 was replaced by alanine (C3478A). This C3478A mutant was utilized in order to determine whether or not the observed processing of p29 was dependent on the proteinase activity of the 3CLpro itself. The cysteine proteinase inhibitor, NEM, was also used for this purpose. *In vitro* transcription–translation of the wild-type pET21-HD1.3C.HD2 in the presence of the inhibitor resulted in a decreased production of the 29-kDa proteinase product (Fig. 3, lane 3). In translation reactions with the C3478A mutant, p29 production was abolished (lane 4). These results demonstrate that the 29-kDa 3CLpro results from its own autocatalytic processing from the flanking domains.

Investigation of membrane requirement

Translation of pET21-HD1.3C.HD2 in the absence of microsomes did not result in appreciable levels of p29 processing in a 90-min *in vitro* reaction. However, when this incubation time was extended to 4 hr, a low level of p29 processing was observed (data not shown). Thus, the presence of microsomes is not an absolute requirement for processing. To further study this observation, the plasmid pET21-HD1.3C.HD2 was *in vitro*-transcribed and translated in the absence or presence of microsomal membranes and the level of p29 production was analyzed by SDS–PAGE at time points between 0 and 300 min (Figs. 4A and 4B). In reactions carried out in the absence of microsomes, p29 could not be detected until after 90 min of translation. In contrast, p29 was detected by 45 min and its levels increased steadily in translation reactions performed in the presence of microsomes. This suggests that while microsomal membranes are not absolutely required for the *in vitro* processing of p29, their presence in the translation reaction can greatly enhance the processing activity of the 3CLpro.

Pulse–chase experiments performed either in the absence or presence of microsomal membranes gave similar results. The 29-kDa proteinase could always be detected at much shorter times in those reactions carried out in the presence of microsomes (data not shown).

We also studied the effect of adding microsomal membranes only after the pulse-labeling period. *In vitro* transcription and translation of pET21-HD1.3C.HD2 was carried out in the absence of microsomal membranes. After a 90-min pulse period, the translation reaction was

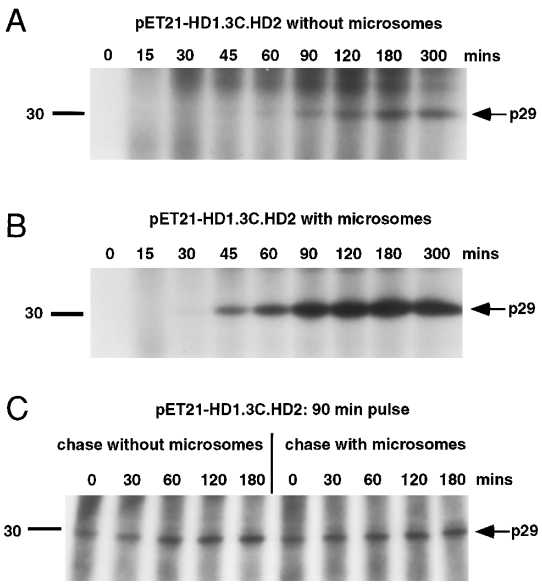

FIG. 4. Synthesis and processing of 3CLpro *in vitro.* The processing efficiency of the 3CLpro in the absence or presence of microsomal membranes was examined by pulse-label analysis. *In vitro* transcription–translation reactions of pET21-HD1.3C.HD2 were prepared either in the absence (A) or presence (B) of microsomes. 5-μl aliquots were removed from each reaction at the indicated time points and analyzed on a 10% SDS–polyacrylamide gel. The effect of adding microsomes to the *in vitro* reaction posttranslationally was also examined (C). Only the regions of interest are shown. The 30-kDa molecular weight protein marker is indicated on the left of each panel. The arrows on the right indicate the electrophoretic mobility of the 29-kDa 3CLpro.

stopped by the addition of cyclohexamide, RNase, and excess cold methionine. The reaction was then divided into two equal volumes and microsomal membranes were added to one half of the reaction. Aliquots were removed at the times indicated during the 180-min chase and analyzed directly by SDS–PAGE. In this experiment, we were able to detect a low level of p29 at the end of the 90-min pulse period (Fig. 4C). This low level of p29 remained constant throughout the entire chase period and did not increase even when the reactions were supplemented with microsomes posttranslationally. This suggests that in order to exert its enhancing effect on the proteolytic processing of the 3CLpro the microsomal membranes have to be present in the reaction cotranslationally.

Determinants of membrane requirement

The role of membranes in the efficient processing of the 3CLpro was further investigated using a series of truncated constructs which encode shorter portions of the surrounding hydrophobic regions. These constructs are schematically represented in Fig. 5A and were all derived from the parental construct pET21-HD1.3C.HD2. The plasmid pET21-HD1.3C.Hind3 encodes a polyprotein carrying a 93-amino acid truncation from the carboxy-terminal end compared to that of the parental construct. This plasmid encodes the amino-terminal hydrophobic domain, HD1, and 3CLpro, like pET21-HD1.3C.HD2, but only 52 residues of the carboxy-terminal hydrophobic domain, HD2. In the construct pET21-HD1.3C, the entire HD2 was deleted whereas in pET21-3C.HD2, all of HD1 from the parental construct was removed.

The results obtained from *in vitro* expression of these constructs are shown in Fig. 5B. In all cases the full-length translation products detected migrated faster than expected from their predicted molecular weights. pET21-HD1.3C.Hind3, pET21-HD1.3C, and pET21-3C.HD2 gave rise to primary translation products with apparent molecular weights of 46, 43, and 37 kDa, respectively (predicted molecular weights 62, 55, and 51 kDa). The parental construct, pET21-HD1.3C.HD2, is shown in lanes 1 and 2 for comparison. As expected, this construct demonstrated a requirement for microsomal membranes in order for the 29-kDa 3CLpro to be efficiently released from the precursor protein. The construct, pET21-HD1.3C.Hind3, containing a partial truncation in HD2, displayed a similar requirement for microsomes as the parental construct (lanes 3 and 4). In the remaining two constructs, pET21-HD1.3C and pET21-3C.HD2, however, this requirement for membranes in the translation reaction was lost (lanes 5 to 8). Equivalent levels of p29 were obtained from reactions that contained or lacked microsomal membranes. Interestingly, these last two constructs encode only one hydrophobic domain, while both the pET21-HD1.3C.HD2 and pET21-HD1.3C.Hind3 constructs encode parts of both hydrophobic domains. It seems therefore, that the requirement for membranes is directly related to having hydrophobic sequences flanking both ends of the proteinase.

Trans proteolytic activity of the *E. coli*-generated recombinant 3CLpro

The enhancement of proteolytic processing in the presence of microsomal membranes could be due to the efficient presentation of the cleavage sites to the 3CLpro by the membranes. Alternatively, the membranes may contribute to the proper folding of the proteinase into an active conformation. To distinguish between these two possibilities, we conducted *in vitro trans* cleavage assays as previously described (Lu *et al.,* 1995) using substrates and enzymes both generated in a coupled transcription–translation system. In these experiments we used radiolabeled translation reactions of the plasmid pET21-HD1.3C.HD2 C3478A, encoding an inactivating mutation in the 3CLpro domain, as substrate. Unlabeled translation reactions of pET21-3C were used as the source of enzyme. However, we were unable to demonstrate *trans* cleavage using this system. A recombinant 3CLpro was subsequently tested *in trans* cleavage assays using radiolabeled substrates generated in the absence or presence of microsomal membranes. The 3CLpro domain

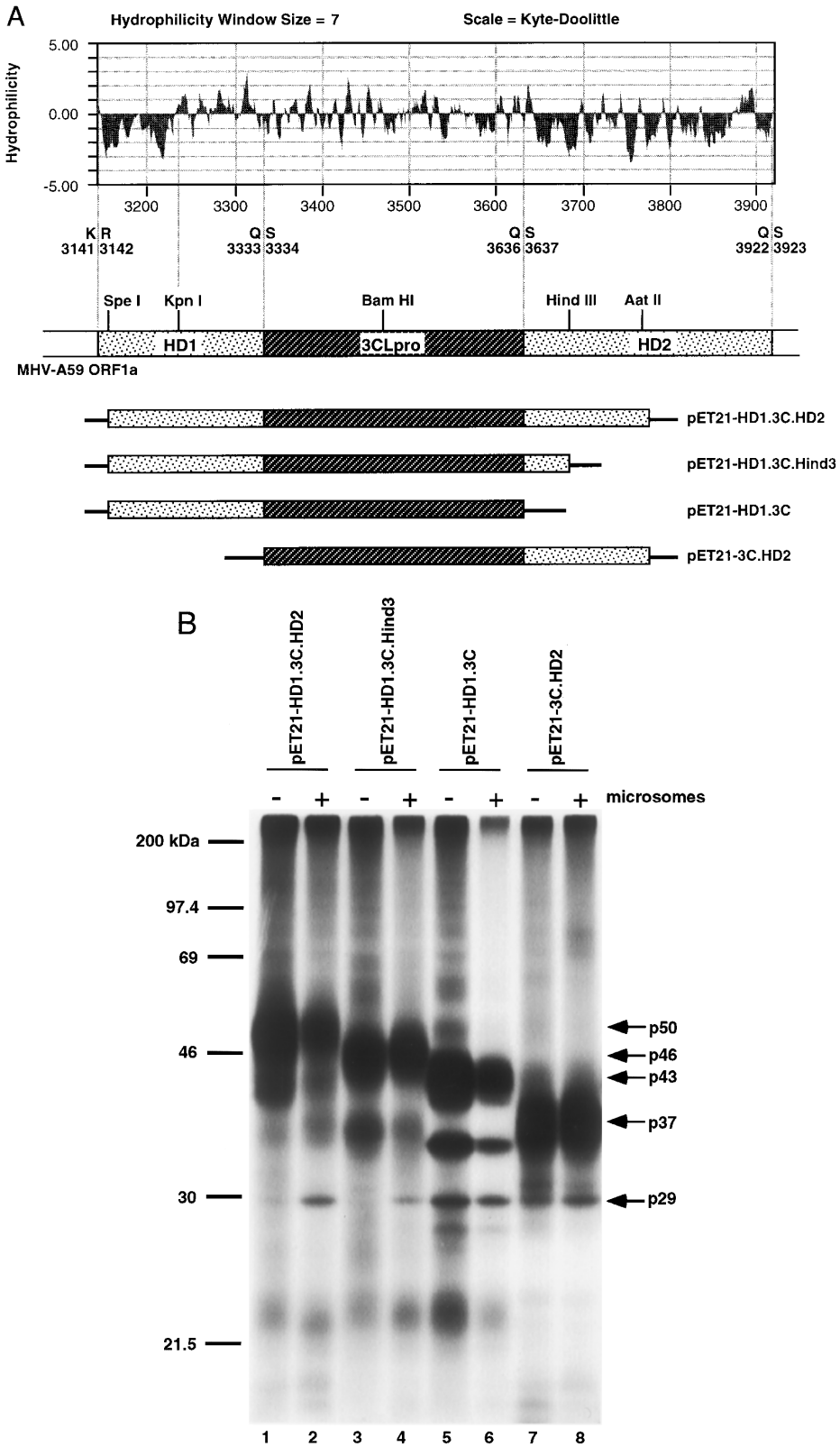

FIG. 5. Relationship between the membrane requirement and the hydrophobic domains. (A) Map of the entire HD1-3CLpro-HD2 region showing a hydrophilicity analysis (MacVector) on the 3CLpro and flanking domains. A schematic representation of the regions of MHV-A59 ORF 1a encoded in the parental construct pET21-HD1.3C.HD2 and all amino- and carboxy-terminal truncation constructs derived from it (see text) are shown. (B) 3CLpro processing by the truncated precursor proteins. The plasmids diagrammed in (A) were *in vitro*-transcribed and translated. Volumes of [^{35}S]methionine-labeled lysates containing equivalent amounts of acid precipitable counts were analyzed directly on a 10% SDS–polyacrylamide gel. Lanes 1 and 2, pET21-HD1.3C.HD2; lanes 3 and 4, pET21-HD1.3C.Hind3; lanes 5 and 6, pET21-HD1.3C; lanes 7 and 8, pET21-3C.HD2. The

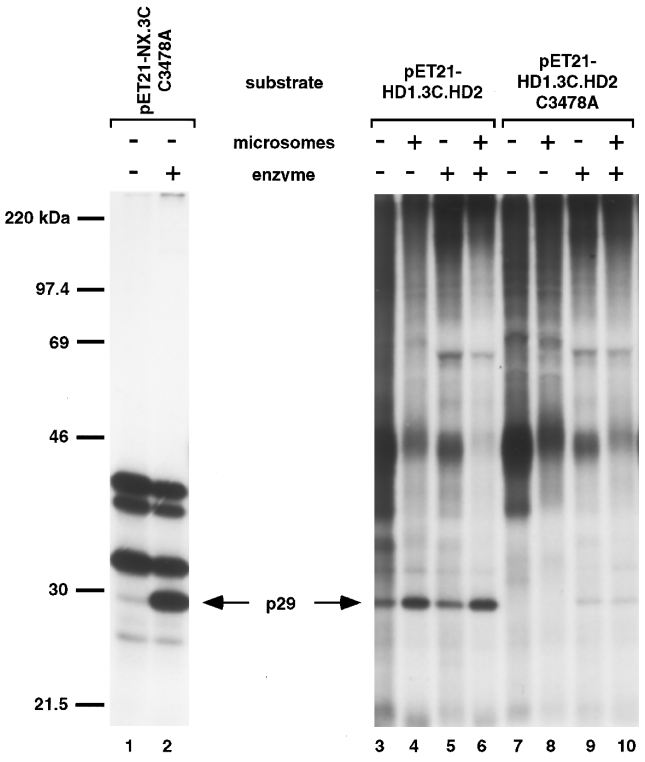

FIG. 6. Postproteolytic *trans* processing. Recombinant 3CLpro was overexpressed and partially purified from *E. coli* and used in postproteolytic *trans* cleavage assays on radiolabeled substrates generated in the absence or presence of microsomes (−/+ microsomes) by the TnT system. Substrate volumes containing equivalent counts per minute were incubated with 3–4 μg of the recombinant 3CLpro or with an equivalent volume of column buffer/20% glycerol (−/+ enzyme) for 12–16 hr at 30°. Lanes 1–2, substrate generated from pET21-NX.3C C3478A; lanes 3–6, substrate generated from pET21-HD1.3C.HD2 containing an active 3CLpro; lanes 7–10, substrate generated from pET21-HD1.3C.HD2 C3478A.

(Ser3334-Gln3636) was overexpressed in, and partially purified from, *E. coli* as part of a fusion protein with the maltose binding protein (MBP). Figure 6 shows the ability of the recombinant MBP-3CLpro fusion proteinase to efficiently cleave an ORF1a protein substrate generated from the plasmid pET21-NX.3C C3478A (lanes 1 and 2). This substrate, which encodes the carboxy-terminal half of HD1 and the entire 3CLpro domain, inactivated by the C3478A mutation, was cleaved *in trans* by the recombinant proteinase resulting in the production of the 29-kDa 3CLpro. To investigate the effect of microsomal membranes on the presentation of the cleavage sites to the enzyme supplied *in trans,* we translated the plasmid pET21-HD1.3C.HD2 C3478A in the absence (lane 7) and presence (lane 8) of microsomes. In the absence of the recombinant 3CLpro, we did not detect any processing from this substrate. The precursor protein was then used as a substrate in a posttranslation proteolytic assay with the recombinant 3CLpro. In the absence of microsomal membranes, the precursor generated from pET21-HD1.3C.HD2 C3478A was processed by the recombinant proteinase, albeit inefficiently (lane 9). The addition of microsomal membranes during translation did not enhance the ability of this precursor to be processed by the recombinant 3CLpro (lane 10). This suggests that membranes are not involved in the presentation of the QS cleavage sites to the exogenously added recombinant proteinase. It is clear, however, that the NX.3C C3478A precursor is much more efficiently cleaved by the recombinant proteinase. This suggests that the presence of the hydrophobic regions in the HD1.3C.HD2 precursor contributes to its inefficiency as a substrate for *trans* cleavage and that this inefficiency is not overcome by the addition of membranes.

We also used the wild-type precursor HD1.3C.HD2, carrying an active 3CLpro, as a substrate for the recombinant proteinase. This precursor, by itself, is able to undergo autoproteolytic cleavage giving rise to the 29-kDa proteinase even in the absence of microsomes (lane 3), during the 16-hr incubation. This processing event is more efficient in the presence of microsomes (lane 4), as expected. The addition of the recombinant 3CLpro to these substrates did not result in an increase in p29 production (lanes 5 and 6), suggesting that the mechanism by which the 29-kDa proteinase is released from the flanking domains involves an autoproteolytic *cis* cleavage.

Membrane association

The hydrophobic nature of the sequences surrounding the 3CLpro, coupled with the prediction that these domains may be membrane spanning, prompted us to investigate the ability of these hydrophobic sequences to interact with the microsomal membranes. We conducted membrane association assays, wherein the microsomal membranes and any attached proteins were separated from the rest of the lysates by a brief centrifugation period at 4°. Following this treatment, the 29-kDa 3CLpro from translation of pET21-HD1.3C.HD2 was present in the soluble fraction, with residual amounts associated with the pellet (Fig. 7, lanes 1 and 2). We were unable to detect p29 in the soluble or pellet fractions of translations carried out using the C3478A mutant (lanes 3 and 4), again confirming that this observed processing is dependent

−/+ signs above each lane indicate the absence or presence of microsomal membranes in the translation reaction. The molecular weight of the protein markers are indicated on the left. Shown on the right are the full-length translation products generated by each construct and the 29-kDa 3CLpro. In addition to a full-length translation product of 43 kDa and the 29-kDa 3CLpro, translation of pET21-HD1.3C also yields another major translation product of 35 kDa. p35 is most likely a product of internal initiation since its synthesis is not inhibited by NEM and it contains the carboxy-terminal end of the 3CLpro as evidenced by its immunoprecipitation by UP313 (data not shown).

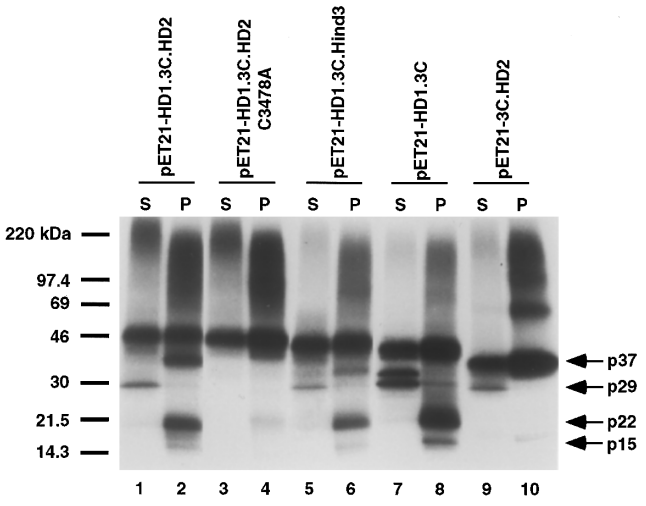

FIG. 7. Membrane association assays. The plasmids pET21-HD1.3C.HD2, pET21-HD1.3C.HD2 C3478A, pET21-HD1.3C.Hind3, pET21-HD1.3C, and pET21-3C.HD2 were *in vitro*-transcribed and translated in the presence of microsomes. Following translation, the soluble (S) and membrane pellet (P) fractions were separated. Fraction volumes containing equivalent counts per minute were analyzed on a 4–20% polyacrylamide gel (Novex). Molecular weight protein markers are indicated on the left. The full-length precursor and processed products are shown on the right.

on the activity of the 3CLpro. In addition, we were able to detect three other polypeptides with molecular weights of approximately 37, 22, and 15 kDa that were present in the pellet fraction of translations with the wild-type construct. These bands were not present in the pellet fraction of translations using the C3478A mutant, suggesting that these are products of processing by the 3CLpro. That these bands are present almost exclusively in the pellet fraction implies that they are associated with the membranes and may therefore represent the fully processed hydrophobic domains or partially processed products containing either hydrophobic domain. In particular, p37 has an electrophoretic migration identical to the precursor protein encoded by the plasmid pET21-3C.HD2. This band, therefore, likely represents a partially processed product containing the 3CLpro and the carboxy-terminal hydrophobic domain.

We have also performed membrane association assays using our truncated constructs (Fig. 7). In all cases, centrifugation of the lysates following *in vitro* translation led to the distribution of the 3CLpro almost exclusively in the soluble fraction of the reactions (lanes 5, 7, and 9). Interestingly, both the p22 and p15 proteins were also detected in the pellet fractions of transcription–translation reactions using pET21-HD1.3C.Hind3 (lane 6) and pET21-HD1.3C (lane 8), but not pET21-3C.HD2 (lane 10). This observation suggests that these two proteins are related to the first hydrophobic domain (HD1) rather than the second (HD2).

In order to identify HD1 from among the processed products, we placed the influenza virus HA epitope immediately upstream of HD1 in the construct pET21-HD1.3C. The resulting plasmid, pET21-HA.HD1.3C, was used in membrane association assays and compared to pET21-HD1.3C. In translation reactions using both plasmids the 3CLpro was located almost exclusively in the soluble fraction of the reactions (Fig. 8, lanes 1 and 3). In the pellet fraction, both p22 and p15 were present in each case (lanes 2 and 4). Immunoprecipitation of the soluble and pellet fractions with the antibody 12CA5 prior to SDS–PAGE analysis revealed the full-length precursor (43 kDa) in the soluble fraction and the 22-kDa protein, as well as the full-length precursor, in the pellet fraction of the pET21-HA.HD1.3C translation reaction (lanes 7 and 8). No proteins were detected upon immunoprecipitation of the soluble and pellet fractions of the pET21-HD1.3C translation reaction with the 12CA5 antibody (lanes 5 and 6) as expected, since this plasmid does not encode the HA epitope. These results unambiguously identify the 22-kDa protein as the amino-terminal hydrophobic domain (HD1) and the 43-kDa protein as the HD1-3CLpro precursor protein. The identity of p15 remains unknown, but it is clear that this protein is related to the 22-kDa HD1 since it is found exclusively in the pellet fraction. The p15 protein may simply represent a degradation product of p22. These observations represent the first demonstration of a physical association between HD1 and membranes for a coronavirus *in vitro.*

DISCUSSION

A common strategy adopted by positive-stranded RNA viruses is the expression of a large polyprotein precursor, followed by the processing of this precursor polyprotein into individual, mature viral proteins. Responsible for these processing events are several viral-encoded proteinases whose significance in viral genomic expression and replication have been well documented (Dougherty and Semler, 1993). For the murine coronavirus, two such viral proteinase activities have been identified. Both the PLP-1 and 3CLpro, whose proteolytic activities have been demonstrated *in vitro* (Baker *et al.,* 1990, 1993; Bonilla *et al.,* 1995; Lu *et al.,* 1995), are encoded as part of the large polyprotein precursor that results from the translation of the viral RNA genome. Flanked by hydrophobic domains, the serine-like proteinase, 3CLpro, is believed to be the principal proteinase responsible for the processing of the large precursor polyprotein into individual, functional replicase proteins. As many as 11 potential 3CLpro cleavage sites have been predicted flanking the potentially important domains encoded in gene 1 (Gorbalenya *et al.,* 1989; Lee *et al.,* 1991). These include cleavage sites that flank the putative polymerase, helicase, and growth factor-like regions as well as cleavage sites surrounding the 3CLpro. Processing at several of these sites has already been demonstrated in several coronaviruses (Grotzinger *et al.,* 1996; Lu *et al.,* 1995;

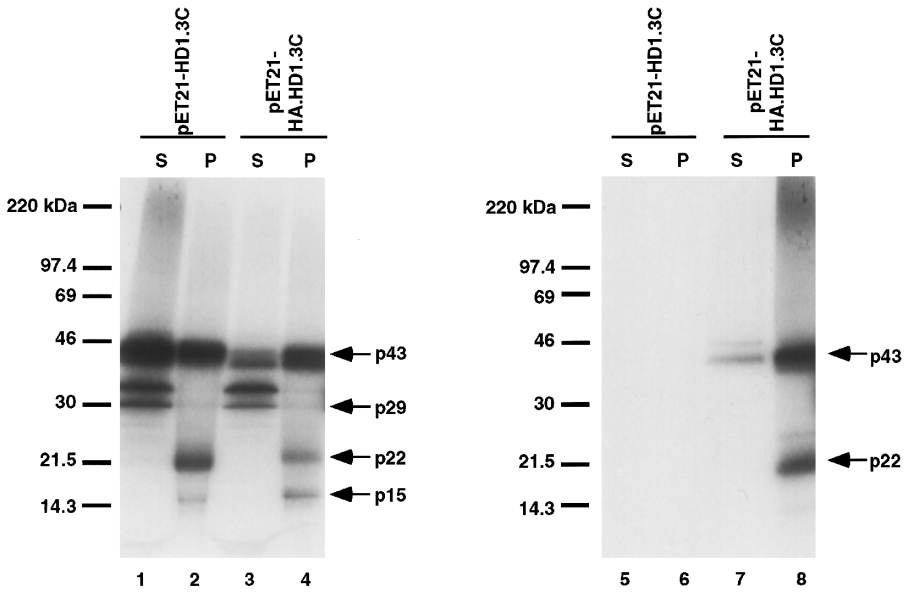

FIG. 8. Epitope tagging of HD1. Membrane association assays were performed using the plasmids pET21-HD1.3C and pET21-HA.HD1.3C, which contains the influenza HA epitope immediately upstream of HD1. Soluble and membrane pellet fractions volumes containing equivalent amounts of [^{35}S]methionine acid precipitable counts per minute were immunoprecipitated with the 12CA5 antibody and analyzed on a 4–20% polyacrylamide gel (Novex). The 35-kDa protein (also seen in Figs. 5B and 7) is present in the soluble fraction of both pET21-HD1.3C and pET21-HA.HD1.3C (lanes 1 and 3). This protein, however, is not immunoprecipitated by 12CA5 (lanes 5 and 7), further supporting the suggestion that this protein is a product of internal initiation (see legend to Fig. 5B).

Tibbles *et al.,* 1996; Ziebuhr *et al.,* 1995). For MHV-A59, the QS dipeptide flanking the N-terminus of the proteinase has been demonstrated to be processed by the 3CLpro *in vitro* (Lu *et al.,* 1995).

In this study, we identified the 3CLpro using an antibody directed against the last 19 amino acids at the carboxy-terminus of the proteinase domain. The 3CLpro was identified from *in vitro* translations of several plasmids encoding the proteinase as part of a precursor polyprotein, and also from lysates of MHV-A59-infected cells. In both cases, the 3CLpro migrated on SDS–polyacrylamide gels as a 29-kDa protein. This is similar in size to, and is presumably the same protein as the previously reported p27 3CLpro (Lu *et al.,* 1995). Because the epitope recognized by the UP313 antibody is at the extreme end of the proteinase domain adjacent to the predicted QS cleavage site at the junction between the 3CLpro and HD2, we are confident that this p29 protein represents the full-length 3CLpro.

We also demonstrate in this report a requirement for microsomal membranes for the efficient processing of the 3CLpro from the flanking hydrophobic sequences. This membrane requirement has not been previously reported for the MHV-A59 3CLpro. However, the 3C-like proteinase of IBV was reported to show an absolute requirement for microsomes for its processing activity *in vitro* (Tibbles *et al.,* 1996). We report here that only when the translation of the pET21-HD1.3C.HD2 plasmid was carried out in the presence of microsomal membranes was the processed p29 readily detectable. Unlike the IBV 3C-like proteinase, however, this requirement for membranes is not absolute for the MHV-A59 3CLpro since extended incubations of the *in vitro* translation of pET21-HD1.3C.HD2 in the absence of microsomal membranes produced low levels of p29 processing. However, their presence in the reaction cotranslationally greatly enhanced the efficiency of p29 processing (Figs. 4A and 4B). This requirement for membranes suggests an interaction between the precursor protein and membranes in order to achieve the proper protein conformation necessary for efficient processing at the flanking QS cleavage sites resulting in the release of the 29-kDa proteinase. Moreover, the inability of microsomal membranes to enhance proteolytic activity posttranslationally suggests that this interaction occurs cotranslationally and may involve the insertion of the hydrophobic domains into the membranes.

The membrane requirement is directly related to the presence of hydrophobic sequences flanking both termini of the 3CLpro. The translation reactions of pET21-HD1.3C and pET21-3C.HD2, constructs encoding only one of the flanking hydrophobic domains, produced similar levels of p29 independent of the presence of microsomal membranes. In pET21-HD1.3C.Hind3, the addition of the first 52 amino acid residues of HD2 to the carboxy-terminal end of pET21-HD1.3C resulted in the loss of the ability to process p29 in the absence of microsomes. These results are consistent with those reported previously for the MHV-A59 3CLpro (Lu *et al.,* 1995), wherein the construct used, pGpro, contained a *Kpn*I–*Hin*dIII frag-

ment of MHV-A59 ORF 1a (see Fig. 5A) that encoded the 3CLpro and portions of the surrounding sequences. Compared to our pET21-HD1.3C.Hind3 construct, pGpro lacks the amino-terminal 87 amino acids representing the hydrophobic residues of HD1. The only hydrophobic sequences encoded in this plasmid flank the carboxy-terminal end of the 3CLpro and, based on our observations, would not be expected to require microsomes for autoproteolysis. Not surprisingly, pGpro did not require the presence of microsomes for *in vitro* activity (Lu *et al.,* 1996, 1995). We speculate that when both termini of the 3CLpro are flanked by hydrophobic sequences, these domains may aggregate together in the absence of membranes in order to shield themselves from the aqueous environment. The amino acid sequences representing the 3CLpro that lie in the middle of this precursor inevitably become misfolded, resulting in an inefficient proteinase. Since precursor proteins with only one hydrophobic domain do not require membranes for processing by the 3CLpro, this suggests that in such precursors the hydrophobic region alone may become misfolded. The rest of the protein, however, may still be able to achieve a conformation that permits processing by the 3CLpro. Hence, in such precursors, membranes are not necessary for proteinase activity.

This speculation is further supported by the observation that a recombinant 3CLpro supplied *in trans* is able to efficiently process a precursor protein generated from the pET21-NX.3C C3478A plasmid which does not encode any hydrophobic sequences. However, the HD1.3C.HD2 C3478A precursor, containing both hydrophobic domains, serves as a very inefficient substrate for the recombinant proteinase. Generating the HD1.3C.HD2 C3478A precursor protein in the presence of microsomal membranes, however, does not increase its efficiency as a substrate for the recombinant 3CLpro, demonstrating that membranes have no effect on *trans* processing by the recombinant 3CLpro. Furthermore, the addition of the recombinant proteinase to the HD1.3C.HD2 substrate in which the proteinase had not been inactivated did not increase the levels of p29 production from these precursors. These results, taken together, strongly suggests that the enhanced processing of the 3CLpro observed in the presence of membranes upon coupled transcription–translation of wild-type precursors, containing both substrate and active enzyme, cannot be attributed to an increase *in trans* cleavage, but rather is due to an enhancement of *cis* processing by the 3CLpro. It is also clear that the microsomes are not required as a cofactor for enzyme activity since the processing of the NX.3C C3478A precursor protein takes place efficiently in the absence of microsomes. These data support our contention that membrane binding plays a role in keeping the entire HD1.3C.HD2 precursor, both substrate and enzyme, in a proper conformation with respect to each other for autocatalytic *cis* processing by the 3CLpro to take place.

One challenging aspect of this study has been the proper identification of the precursor polyproteins as well as all processed products, partial or complete. It has been our experience that these precursors migrate on SDS–polyacrylamide gels with electrophoretic mobilities faster than that predicted based on their primary amino acid sequence. This apparent conflict between the predicted and observed molecular weights of the precursor and processed proteins was previously reported in investigations of both the HCV 229E (Ziebuhr *et al.,* 1995) and MHV-A59 3C-like proteinases (Lu *et al.,* 1995). The observed molecular weight of the 3CLpro itself, 29 kDa, is smaller than its predicted molecular weight of 33 kDa. Furthermore, each of the 3CLpro-encoding plasmids used in our study resulted in primary translation products with electrophoretic mobilities faster than expected. It is therefore difficult to positively identify all precursor and processed products based solely on their apparent molecular weights without the benefit of having a panel of antibodies directed against these regions under study. We were able to positively identify the 3CLpro using a antipeptide antibody directed at the carboxy-terminal end of the proteinase. However, such antibodies are not, at present, available for either of the hydrophobic domains. Instead, we placed an epitope (HA-) tag immediately upstream of the HD1 in the construct pET21-HA.HD1.3C and used the 12CA5 antibody directed against this epitope to unambiguously identify the precursor protein encoded by this plasmid. This precursor migrated with an apparent molecular weight of 43 kDa, faster than its predicted molecular weight of 55 kDa. Using the HA-tag the processing product corresponding to the amino-terminal hydrophobic domain was also identified in association with membranes upon expression of this plasmid *in vitro.* This is the first *in vitro* demonstration of a physical interaction between this amino-terminal hydrophobic domain and membranes. However, in such an analysis the nature of this interaction, whether peripheral or integral, cannot be discerned. We estimated that approximately 37% of the total translated proteins becomes associated with membranes (data not shown). This number is variable and seems to be independent of the hydrophobic content of the precursor protein, that is to say, increasing hydrophobic content of the precursor does not correlate with a greater partitioning into the membranes. Instead, this calculation may reflect the capacity of the microsomes to take in proteins or the fact that the microsomes may be a limiting reagent in these *in vitro* reactions. Preliminary studies show that the hydrophobic domains and hydrophobic-containing precursors remain in the membranes following alkali extraction (Mostov *et al.,* 1981) to the same extent as the coro-

navirus S protein under the same conditions (data not shown). These results suggest that portions of the hydrophobic domains may be membrane spanning.

We have not yet been able to identify a protein band corresponding to the carboxy-terminal hydrophobic domain (HD2). The predicted molecular weight of HD2 is approximately 17 kDa. However, since it has been our experience that the proteins encoded in this region of ORF 1a do not migrate with their expected electrophoretic mobilities, it would not be surprising if HD2 migrated with a much faster electrophoretic mobility than expected.

The presence of hydrophobic sequences flanking the 3CLpro suggests a role for these domains not only in the proper folding of the precursor protein, but also in the localization of this region of the gene 1 polyprotein to a target organelle during coronavirus infection. In the arterivirus, equine arteritis virus (EAV), which is evolutionarily related to the coronavirus-like superfamily (den Boon *et al.,* 1991), it has recently been demonstrated that the proteolytic products of ORF 1b generated by the EAV nsp4 proteinase are localized to a membranous compartment of the host cell during viral infection (Van Dinten *et al.,* 1996). The nsp4 proteinase is a chymotrypsin-like serine proteinase belonging to the group of 3C-like serine proteases (Snijder *et al.,* 1996). Similar to the 3C-like proteinases of coronaviruses, two transmembrane hydrophobic domains are predicted to reside on either side of the 3C-like nsp4 proteinase domain (Snijder *et al.,* 1994). Based on the accumulating evidence in EAV, it has been suggested that the replicase cleavage products assemble into a large replication complex that is anchored in the membrane through these hydrophobic regions (Van Dinten *et al.,* 1996). The replication complexes of numerous positive-stranded RNA viruses have been found to be membrane associated (Bienz *et al.,* 1994, 1992; Chambers *et al.,* 1990; Froshauer *et al.,* 1988; Van Dinten *et al.,* 1996). Thus, it is plausible that in MHV-A59-infected cells the protein domains encoded by the replicase gene are targeted to certain membranous organelles. In support of this idea, we have demonstrated that the PLP-1 is localized to the Golgi apparatus during MHV infection (Bi *et al.,* 1995). We are currently investigating whether or not the 3CL pro of MHV-A59 is also localized to membranes *in vivo.*

ACKNOWLEDGMENTS

The authors thank Xinhe Jiang and Xiurong Wang for their excellent technical assistance and Dr. Michael Malim for providing the 12CA5 antibody. This work was supported by Public Health Service Grant AI-17418. J.D.P. was supported in part by Merck and AI-17418. J.D.T. was supported in part by Merck and Training Grant AI-07325. P.J.B. was supported by a supplement for underrepresented minorities for Public Health Service Grant NS-21954.

REFERENCES

Baker, S. C., La Monica, N., Shieh, C. K., and Lai, M. M. (1990). Murine coronavirus gene 1 polyprotein contains an autoproteolytic activity. *Adv. Exp. Med. Biol.* 276, 283–289.

Baker, S. C., Yokomori, K., Dong, S., Carlisle, R., Gorbalenya, A. E., Koonin, E. V., and Lai, M. M. (1993). Identification of the catalytic sites of a papain-like cysteine proteinase of murine coronavirus. *J. Virol.* 67, 6056–6063.

Bi, W., Bonilla, P. J., Holmes, K. V., Weiss, S. R., and Leibowitz, J. L. (1995). Intracellular localization of polypeptides encoded in mouse hepatitis virus open reading frame 1a. *Adv. Exp. Med. Biol.* 380, 251–258.

Bienz, K., Egger, D., and Pfister, T. (1994). Characteristics of the poliovirus replication complex. *Arch. Virol.—Supplementum* 9, 147–157.

Bienz, K., Egger, D., Pfister, T., and Troxler, M. (1992). Structural and functional characterization of the poliovirus replication complex. *J. Virol.* 66, 2740–2747.

Bonilla, P. J., Gorbalenya, A. E., and Weiss, S. R. (1994). Mouse hepatitis virus strain A59 RNA polymerase gene ORF 1a: heterogeneity among MHV strains. *Virology* 198, 736–740.

Bonilla, P. J., Hughes, S. A., Piñón, J. D., and Weiss, S. R. (1995). Characterization of the leader papain-like proteinase of MHV-A59: identification of a new in vitro cleavage site. *Virology* 209, 489–497.

Bonilla, P. J., Hughes, S. A., and Weiss, S. R. (1997). Characterization of a second cleavage site and demonstration of activity in trans by the papain-like proteinase of the murine coronavirus MHV-A59. *J. Virol.* 71, 900–909.

Boursnell, M. E., Brown, T. D., Foulds, I. J., Green, P. F., Tomley, F. M., and Binns, M. M. (1987). Completion of the sequence of the genome of the coronavirus avian infectious bronchitis virus. *J. Gen. Virol.* 68, 57–77.

Bredenbeek, P. J., Pachuk, C. J., Noten, A. F., Charite, J., Luytjes, W., Weiss, S. R., and Spaan, W. J. (1990). The primary structure and expression of the second open reading frame of the polymerase gene of the coronavirus MHV-A59; a highly conserved polymerase is expressed by an efficient ribosomal frameshifting mechanism. *Nucleic Acids Res.* 18, 1825–1832.

Chambers, T. J., Hahn, C. S., Galler, R., and Rice, C. M. (1990). Flavivirus genome organization, expression, and replication. [Review]. *Annu. Rev. Microbiol.* 44, 649–688.

den Boon, J. A., Snijder, E. J., Chirnside, E. D., de, V. A. A., Horzinek, M. C., and Spaan, W. J. (1991). Equine arteritis virus is not a togavirus but belongs to the coronaviruslike superfamily. *J. Virol.* 65, 2910–2920.

Denison, M. R., Zoltick, P. W., Leibowitz, J. L., Pachuk, C. J., and Weiss, S. R. (1991). Identification of polypeptides encoded in open reading frame 1b of the putative polymerase gene of the murine coronavirus mouse hepatitis virus A59. *J. Virol.* 65, 3076–3082.

Dougherty, W. G., and Semler, B. L. (1993). Expression of virus-encoded proteinases: functional and structural similarities with cellular enzymes. [Review]. *Microbiol. Rev.* 57, 781–822.

Echeverri, A. C., and Dasgupta, A. (1995). Amino terminal regions of poliovirus 2C protein mediate membrane binding. *Virology* 208, 540–553.

Eleouet, J.-F., Rasschaert, D., Lambert, P., Levy, L., Vende, P., and Laude, H. (1995). Complete sequence (20 kb) of the polyprotein-encoding gene 1 of transmissible gastroenteritis virus. *Virology* 206, 817–822.

Froshauer, S., Kartenbeck, J., and Helenius, A. (1988). Alphavirus RNA replicase is located on the cytoplasmic surface of endosomes and lysosomes. *J. Cell. Biol.* 107, 2075–2086.

Gorbalenya, A. E., Koonin, E. V., Donchenko, A. P., and Blinov, V. M. (1989). Coronavirus genome: prediction of putative functional domains in the non-structural polyprotein by comparative amino acid sequence analysis. *Nucleic Acids Res.* 17, 4847–4861.

Grotzinger, C., Heusipp, G., Ziebuhr, J., Harms, U., Suss, J., and Siddell,

S. G. (1996). Characterization of a 105-kDa polypeptide encoded in gene 1 of the human coronavirus HCV 229E. *Virology* 222, 227–235.

Herold, J., Raabe, T., Schelle-Prinz, B., and Siddell, S. G. (1993). Nucleotide sequence of the human coronavirus 229E RNA polymerase locus. *Virology* 195, 680–691.

Kim, J. C., Spence, R. A., Currier, P. F., Lu, X., and Denison, M. R. (1995). Coronavirus protein processing and RNA synthesis is inhibited by the cysteine proteinase inhibitor E64d. *Virology* 208, 1–8.

Kolodziej, P. A., and Young, R. A. (1991). Epitope tagging and protein surveillance. *Methods Enzymol.* 194, 508–519.

Lee, H. J., Shieh, C. K., Gorbalenya, A. E., Koonin, E. V., La, M. N., Tuler, J., Bagdzhadzhyan, A., and Lai, M. M. (1991). The complete sequence (22 kilobases) of murine coronavirus gene 1 encoding the putative proteases and RNA polymerase. *Virology* 180, 567–582.

Lu, X., Lu, Y., and Denison, M. R. (1996). Intracellular and in vitro-translated 27-kDa proteins contain the 3C-like proteinase activity of the coronavirus MHV-A59. *Virology* 222, 375–382.

Lu, Y., Lu, X., and Denison, M. R. (1995). Identification and characterization of a serine-like proteinase of the murine coronavirus MHV-A59. *J. Virol.* 69, 3554–3559.

Mostov, K. E., DeFoor, P., Fleischer, S., and Blobel, G. (1981). Co-translational membrane integration of calcium pump protein without signal sequence cleavage. *Nature* 292, 87–88.

Pachuk, C. J., Bredenbeek, P. J., Zoltick, P. W., Spaan, W. J., and Weiss, S. R. (1989). Molecular cloning of the gene encoding the putative polymerase of mouse hepatitis coronavirus, strain A59. *Virology* 171, 141–148.

Snijder, E. J., Wassenaar, A. L., and Spaan, W. J. (1994). Proteolytic processing of the replicase ORF1a protein of equine arteritis virus. *J. Virol.* 68, 5755–5764.

Snijder, E. J., Wassenaar, A. L., van, D. L. C., Spaan, W. J., and Gorbalenya, A. E. (1996). The arterivirus nsp4 protease is the prototype of a novel group of chymotrypsin-like enzymes, the 3C-like serine proteases. *J. Biol. Chem.* 271, 4864–4871.

Tibbles, K. W., Brierley, I., Cavanagh, D., and Brown, T. D. (1996). Characterization in vitro of an autocatalytic processing activity associated with the predicted 3C-like proteinase domain of the coronavirus avian infectious bronchitis virus. *J. Virol.* 70, 1923–1930.

Van Dinten, L. C., Wassenaar, A. L., Gorbalenya, A. E., Spaan, W. J., and Snijder, E. J. (1996). Processing of the equine arteritis virus replicase ORF1b protein: identification of cleavage products containing the putative viral polymerase and helicase domains. *J. Virol.* 70, 6625–6633.

Ziebuhr, J., Herold, J., and Siddell, S. G. (1995). Characterization of a human coronavirus (strain 229E) 3C-like proteinase activity. *J. Virol.* 69, 4331–4338.